ACS Chemical Neuroscience

Research Article

pubs.acs.org/chemneuro

The Potential of Indole and a Synthetic Derivative for PolyQ Aggregation Reduction by Enhancement of the Chaperone and Autophagy Systems

Chih-Hsin Lin,[†,§] Yih-Ru Wu,[§] Pin-Jui Kung,[†] Wan-Ling Chen,[§] Li-Ching Lee,[†] Te-Hsien Lin,[†] Chih-Ying Chao,[§] Chiung-Mei Chen,[§] Kuo-Hsuan Chang,[§] Donala Janreddy,[‡] Guey-Jen Lee-Chen,*[,†] and Ching-Fa Yao*[,‡]

[†]Department of Life Science and [‡]Department of Chemistry, National Taiwan Normal University, Taipei 11677, Taiwan

[§]Department of Neurology, Chang Gung Memorial Hospital, Chang Gung University College of Medicine, Taipei 10507, Taiwan

ABSTRACT: In polyglutamine (polyQ)-mediated disorders, the expansion of translated CAG repeats in the disease genes result in long polyQ tracts in their respective proteins, leading to intracellular accumulation of aggregated polyQ proteins, production of reactive oxygen species, and cell death. The molecular chaperones act in preventing protein misfolding and aggregation, thus inhibiting a wide range of harmful downstream events. In the circumstance of accumulation of aggregated polyQ proteins, the autophagic pathway is induced to degrade the misfolded or aggregated proteins. In this study, we used Flp-In 293/SH-SY5Y cells with inducible SCA3 ATXN3/Q_{75}-GFP expression to test the effect of indole and synthetic derivatives for neuroprotection. We found that ATXN3/Q_{75} aggregation can be significantly prohibited in Flp-In 293 cells by indole and derivative NC001-8. Meanwhile, indole and NC001-8 up-regulated chaperones and autophagy in the same cell models. Both of them further promote neurite outgrowth in neuronal differentiated SH-SY5Y ATXN3/Q_{75}-GFP cells. Our results demonstrate how indole and derivative NC001-8 are likely to work in reduction of polyQ-aggregation and provide insight into the possible effectual mechanism of indole compounds in polyQ spinocerebellar ataxia (SCA) patients. These findings may have therapeutic applications in a broad range of clinical situations.

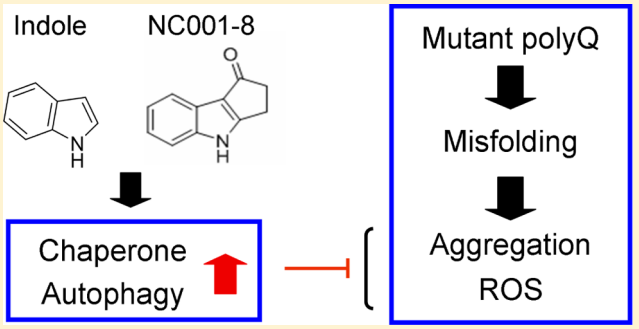

KEYWORDS: *Spinocerebellar ataxia, polyQ expansion, indole and derivative, therapeutics*

Dominantly inherited spinocerebellar ataxias (SCAs) including SCA types 1, 2, 3, 6, 7, 8, and 17 and dentatorubropallidoluysian atrophy (DRPLA) are caused by the expansions of CAG trinucleotide repeats and associated polyglutamine (polyQ) stretch.[1−8] A common feature of polyQ diseases is the accumulation of insoluble intracellular deposits containing the aggregated disease proteins,[9] leading to a gain of function that induces progressive neuronal dysfunction and succeeding degenerative processes.[10] Because misfolding and subsequent accumulation of the mutated polyQ protein are likely the initial events in the pathogenic cascade, suppression of protein misfolding and clearance of aggregated protein are expected to inhibit a wide range of downstream detrimental events and to rescue neuronal dysfunction.

Among the polyQ-mediated SCA, SCA type 3 (SCA3, also known as Machado−Joseph disease, MJD) is the most common form of SCA worldwide,[11] including among ethnic Chinese in Taiwan.[12,13] The disease is characterized by a CAG triplet expansion that has been mapped to chromosome 14q32.12 (ATXN3 gene), which has from 13 to 36 repeats in normal individuals and from 68 to 79 repeats in most of the clinically diagnosed patients.[3] Although full-length ATXN3 protein containing an extended polyQ segment does not readily aggregate on its own, the removal of the N-terminus of polyQ-expanded ATXN3 is required for aggregate formation *in vitro* and *in vivo*.[14] The coaggregation of nonpathogenic ATXN3 protein with polyQ-expanded ATXN3 fragments and the corresponding reduction of intracellular soluble ATXN3 levels could in turn impair ATXN3 function, contributing to the SCA3 pathogenesis.[14]

Indole is an aromatic heterocyclic organic compound. Its derivatives are potent anticancer agents widely studied in treating cancers.[15−18] On the other hand, their potential in neurodegenerative diseases has not been well-known. Previously an endogenous melatonin-related indole structure, indole-3-propionic acid (IPA), was shown to display potent neuroprotective properties against the Alzheimer's β-amyloid.[19] Another endogenous indole derivative, indolepropionamide (IPAM), was also reported to protect rodent mitochondria and extend rotifer lifespan.[20] In this study, we found an

Received: April 10, 2014
Revised: August 27, 2014
Published: September 8, 2014

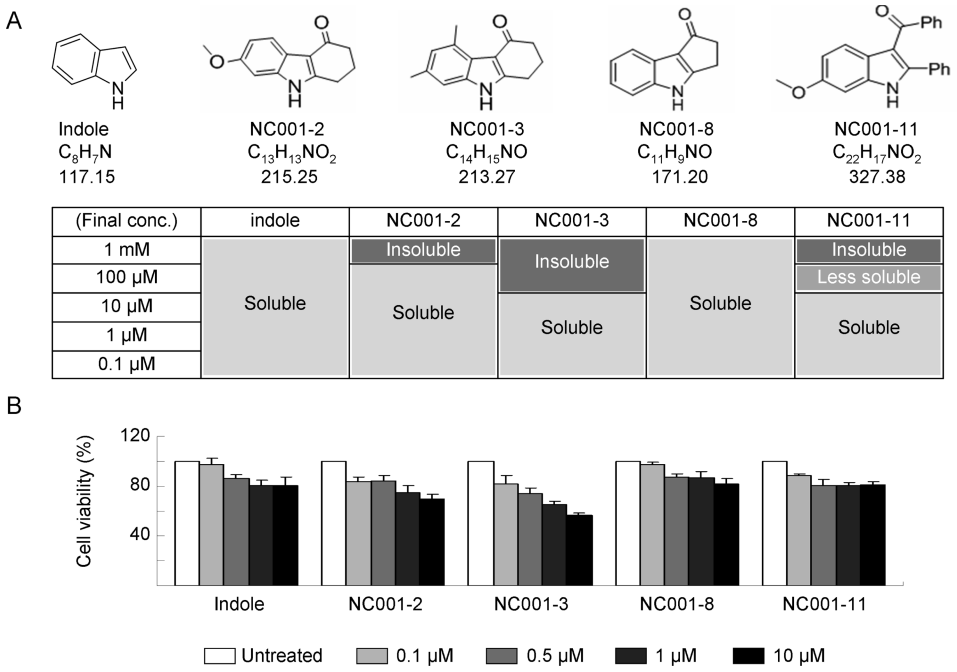

Figure 1. Indole compounds and cytotoxicity. (A) Structure, formula, molecular weight, and solubility (in medium) of studied synthetic indole compounds. (B) Cytotoxicity of indole compounds against 293 cells using MTT viability assay. Cells were treated with 0.1−10 μM indole and derivatives and cell proliferation was measured the next day (n = 3). To normalize, the relative viability in untreated cells is set as 100%.

antiaggregation effect of indole and synthetic derivative NC001-8 in the SCA3 ATXN/Q_{75} cell model by enhancing chaperone and autophage systems and suppressing the production of reactive oxidative species (ROS). The findings provide evidence that indole and its synthetic derivative NC001-8 may have therapeutic potential in polyQ-mediated diseases.

RESULTS AND DISCUSSION

Indole Compounds and IC_{50} Cytotoxicity. Indole has a bicyclic structure, consisting of a six-membered benzene ring fused to a five-membered nitrogen-containing pyrrole ring. Indole is the precursor to many pharmaceuticals, and many indole-containing compounds play an important role in medicine. Previously we showed that novel synthetic indole compound 1,1,3-tri(3-indolyl)cyclohexane inhibits cancer cell growth in lung cancer cells and xenograft models.[21] Because indole compound indomethacin was reported to suppress polyQ aggregation in a cellular model of spinal and bulbar muscular atrophy,[22] indole and randomly selected synthetic derivatives[23] were tested for their potentials to reduce the ATXN3/Q_{75} aggregation on a SCA3 cell model.[24] Based on this preliminary screen (data not shown), indole and four tested derivatives (Figure 1A) were chosen for further studies.

The solubility of these compounds in culture medium was first examined. After vortex mixing and centrifugation (13 000 rpm for 5 min), indole and four tested derivatives were completely soluble in medium from 0.1 to 10 μM (Figure 1A). MTT assays were performed with human embryonic kidney 293 cells after treatment with indole compounds (0.1−10 μM) for 24 h. Indole and derivatives NC001-8 and NC001-11 had at least 80% cell viability up to the tested 10 μM, suggesting their low cytotoxicity (Figure 1B).

Indole Compounds Reduce ATXN3/Q_{75} Aggregation on 293 Cell Model. ATXN3/Q_{75} cells were treated with tested compounds (0.1−1 μM) for 8 h, and doxycycline (Dox) (10 μg/mL) and oxaliplatin (5 μM) were added to induce ATXN3/Q_{75}-GFP expression and to inhibit DNA synthesis, respectively (Figure 2A). The timing for 6 days' induction, which reflected suitable cell density, viability, and aggregate accumulation was optimized. Geranylgeranylacetone (GGA), a potent heat shock protein (HSP) inducer,[25] was included for comparison. Representative fluorescence microscopy images of aggregation after treatment with indole and NC001-8 are shown in Figure 2B. While almost all cells displayed GFP fluorescence, about 15−20% of cells exhibited polyQ aggregates. Aggregation was quantified by Transfluor technology[26] based on GFP intensity. The number of cells that formed aggregates correlated with GFP intensity. As a positive control, HSP inducer GGA reduced the ATXN3/Q_{75} aggregation (or inclusion body formation) to 85% (at 0.1 μM, P = 0.023) compared with untreated cells (100%, Figure 2C). In ATXN3/Q_{75} cells, GGA at 0.5−1 μM may induce ER stress and lead to increased polyQ aggregation, as suggested by triggering unfolded protein response in various cell types.[27] Both indole and derivatives NC001-2, NC001-3, NC001-8, and NC001-11 display good aggregation-inhibitory potential at 0.1−1 μM (73−79% for indole, P = 0.005−0.001; 70−84% for NC001-8, P = 0.009−0.001), 0.1−0.5 μM (84−73% for NC001-2, P = 0.008−0.003; 84−83% for NC001-3, P = 0.014−0.005), or 0.1 μM (74% for NC001-11, P = 0.003) compared with untreated cells.

To examine whether indole, NC001-8, and GGA potentially affect ATXN3/Q_{75}-GFP expression, Western blots were performed using GFP antibody. As shown in Figure 2D, similar expression levels were observed with or without indole, NC001-8, or GGA addition. However, when the protein samples were subjected to filter trap assay and stained with GFP antibody, SDS-insoluble aggregates were evidently reduced in samples treated with indole, NC001-8, and GGA (0.1 μM) (79−87% vs 100%, P = 0.046−0.023).

dx.doi.org/10.1021/cn500075u | ACS Chem. Neurosci. 2014, 5, 1063−1074

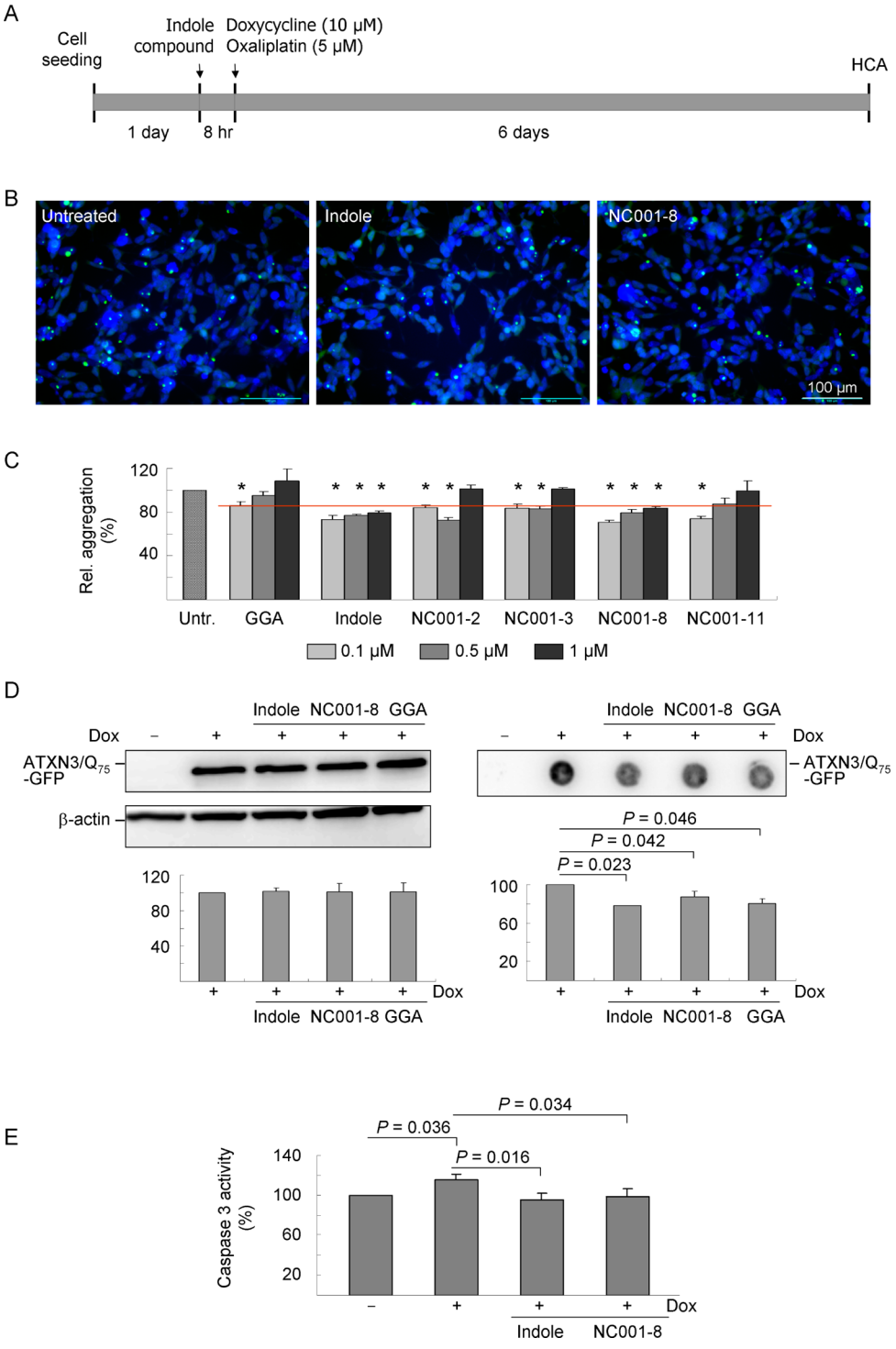

Figure 2. High-content aggregation analysis using Flp-In 293 cells expressing ATXN3/Q_{75}. (A) Experiment flowchart. ATXN3/Q_{75}-GFP 293 cells were plated into 96-well dishes, grown for 24 h, and treated with indole compounds for 8 h. Then doxycycline and oxaliplatin were added to the medium for 6 days, and aggregation percentage was assessed by the high content analysis system. (B) Representative fluorescence microscopy images of ATXN3/Q_{75}-GFP cells untreated or treated with indole or NC001-8 (0.1 μM) for 6 days. Nuclei were counterstained with DAPI (blue). (C) Aggregation analysis (n = 3) of ATXN3/Q_{75}-GFP cells untreated or treated with GGA, indole, NC001-2, NC001-3, NC001-8, and NC001-11 (0.1–1 μM). To normalize, the relative aggregation level in untreated cells is set as 100%. The red line represents 85% aggregation for 0.1 μM GGA treatment. *P < 0.05 between compound-treated and untreated. (D) Western blot analysis and filter trap assay of ATXN3/Q_{75}-GFP cells untreated or treated with indole, NC008-1, or GGA (0.1 μM). After 6 days, total proteins (left) and SDS-insoluble aggregates (right) were probed with GFP antibody to detect total and trapped ATXN3/Q_{75}-GFP. (E) Caspase 3 activity analysis (n = 3) of ATXN3/Q_{75}-GFP cells untreated (+ Dox only) or treated with indole and NC001-8 (0.1 μM). To normalize, the relative caspase 3 activity in uninduced cells (− Dox) is set as 100%.

The protective effect of indole and NC001-8 against polyQ toxicity was further examined using caspase 3 activity assay after induction of ATXN3/Q_{75}-GFP expression for 6 days. As shown in Figure 2E, while significantly increased caspase 3 activity was

dx.doi.org/10.1021/cn500075u | ACS Chem. Neurosci. 2014, 5, 1063–1074

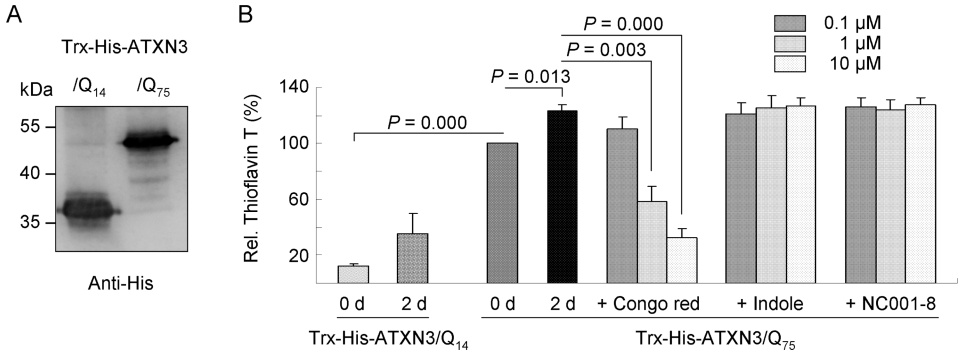

Figure 3. Trx-His-ATXN3/Q_{14-75} proteins and thioflavin T binding assay. (A) Western blot analysis of Trx-His-ATXN3/Q_{14-75} proteins purified from IPTG-induced bacterial cells using anti-His antibody. (B) Thioflavin T binding assay for Trx-His-ATXN3 aggregation. ATXN3 proteins (2.5 μM) was incubated with congo red, indole, or NC001-8 (0.1−10 μM) at 37 °C for 48 h, and aggregation was monitored by measuring thioflavin T fluorescence intensity (n = 3). To normalize, the relative thioflavin T fluorescence of Trx-His-ATXN3/Q_{75} protein without 2 days' incubation at 37 °C is set as 100%.

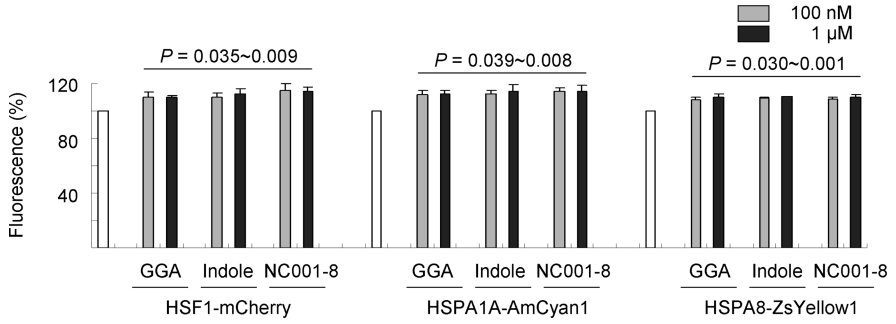

Figure 4. Enhancement of chaperone expression by indole and NC001-8 in 293 cells. Triple fluorescent reporter cells with mCherry, AmCyan1, and ZsYellow1 reporters downstream of HSF1, HSPA1A, and HSPA8 promoters[24] were treated with GGA, indole, or NC001-8 (0.1−1 μM) for 24 h and fluorescence analyzed (n = 3). To normalize, the fluorescence level in untreated cells is set as 100%.

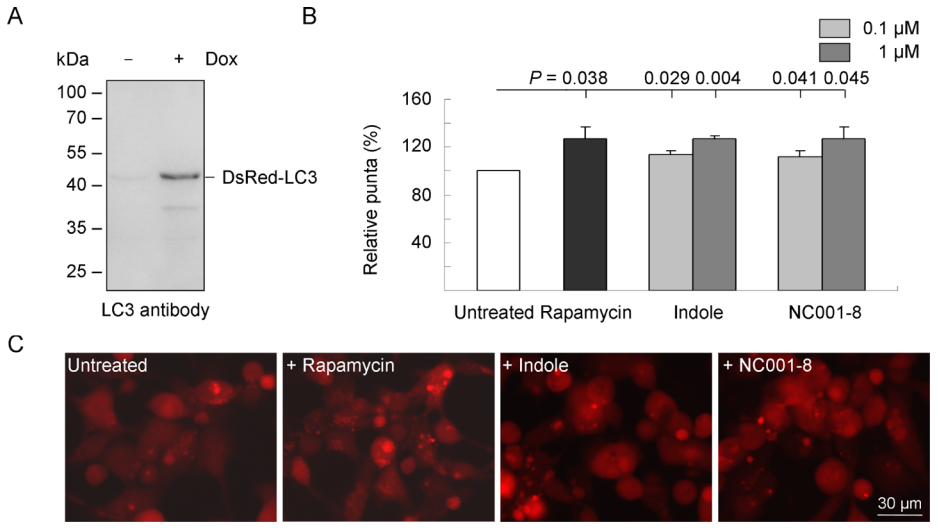

Figure 5. Enhancement of autophagy by indole and NC001-8 in 293 cells. (A) Western blot analysis of DsRed-LC3 protein level using LC3 antibody after 2 days induction with doxycycline (+ Dox). (B) After induction of DsRed-LC3 expression for 1 day, cells were treated with rapamycin (0.2 μM), indole, or NC001-8 (0.1−1.0 μM) for 24 h and punta analyzed (n = 3). To normalize, the relative punta level in untreated cells is set as 100%. (C) Typical morphological changes of autophagosome in DsRed-LC3 cells untreated or treated with rapamycin (0.2 μM), indole, and NC001-8 (0.1 μM).

seen in cells with ATXN3/Q_{75}-GFP expression induced for 6 days (+ Dox) compared with uninduced cells (116% vs 100%, P = 0.036); treatment with indole and NC001-8 (0.1 μM) significantly reduced caspase 3 activity compared with untreated cells (indole 95% vs 116%, P = 0.016; NC001-8 99% vs. 116%, P = 0.034). Taken together, these results suggest that indole and NC001-8 interfere with ATXN3/Q_{75} aggregate formation and reduce aggregate-associated caspase 3 activity.

Indole Compounds Have No Inhibition on PolyQ Aggregation by Thioflavin T Fluorescence Assay. To

dx.doi.org/10.1021/cn500075u | ACS Chem. Neurosci. 2014, 5, 1063−1074

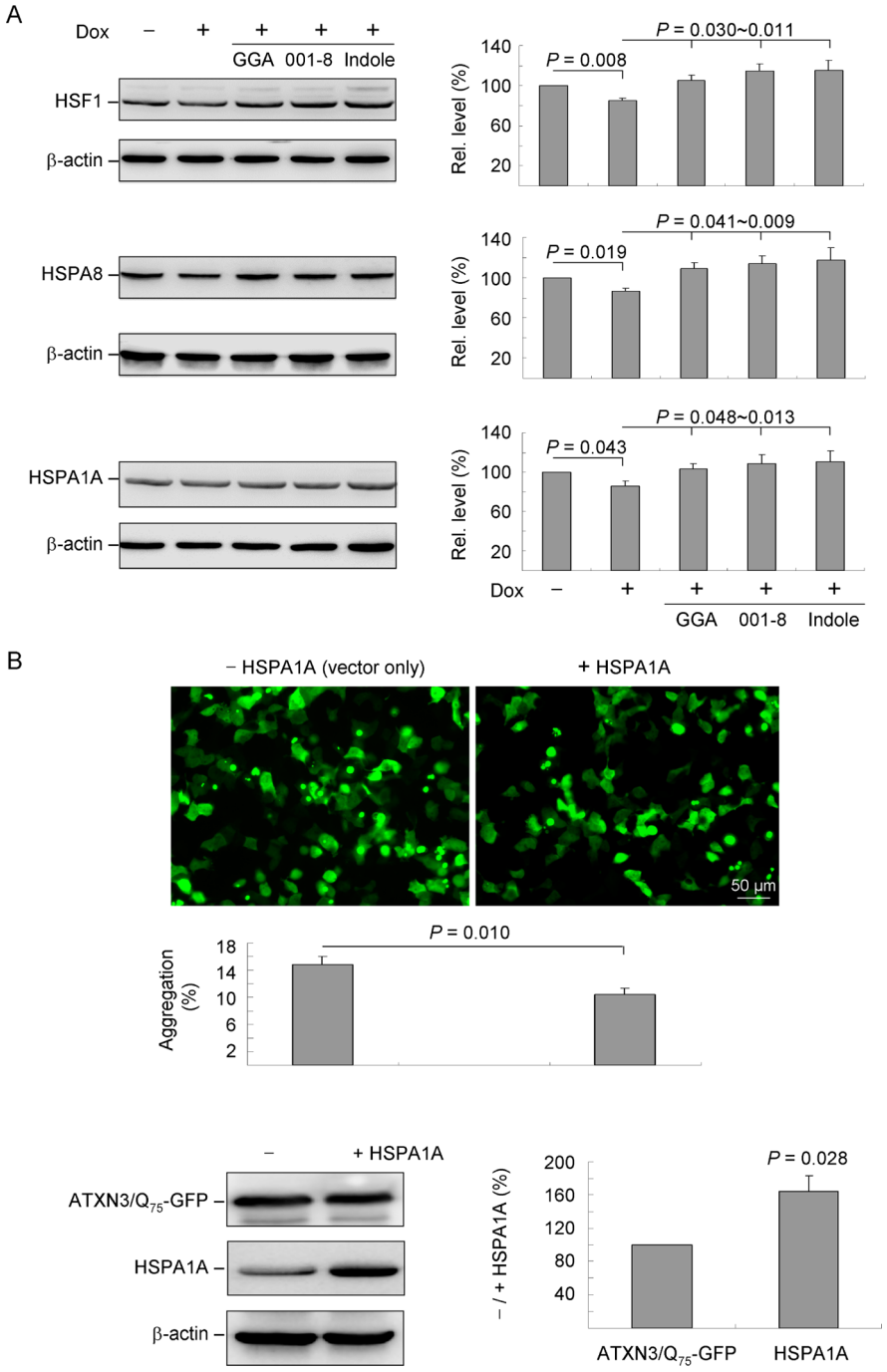

Figure 6. Indole and NC001-8 enhanced chaperone expression on ATXN3/Q_{75} 293 cells and HSPA1A overexpression reduced ATXN3/Q_{75} aggregation. (A) ATXN3/Q_{75} 293 cells were pretreated with GGA, indole, or NC001-8 (0.1 μM) for 8 h, and ATXN3/Q_{75}-GFP expression was induced for 6 days. Relative HSF1, HSPA8, and HSPA1A expressions were analyzed by Western blot analysis using β-actin as a loading control. (B) HEK-293T cells were cotransfected with plasmid encoding ATXN3/Q_{75}-GFP and plasmid with (+HSPA1A) or without (−HSPA1A) HSPA1A cDNA. After 2 days, aggregation percentage was assessed by the HCA system, with the percentage of aggregate formation (ATXN3/Q_{75} green spots) counted among three random fields. Data are expressed as the mean ± SD values from three independent experiments. In addition, cell lysates were prepared, and proteins were analyzed with anti-GFP, anti-HSPA1A, or anti-β-actin antibody.

examine indole and NC001-8 in regulating polyQ aggregation, ATXN3/Q_{14-75} proteins fused to thioredoxin (Trx) and His tags were prepared (Figure 3A). Congo red, a potent polyQ aggregate inhibitor,[28] was included for comparison. When aggregate formation was measured with fluorescence generated by thioflavin T binding, Trx-His-ATXN3/Q_{75} aggregated promptly as compared with Trx-His-ATXN3/Q_{14} (100% vs 12%, P = 0.000) (Figure 3B). Significantly increased ATXN3/Q_{75} aggregation was observed after 2 days' incubation at 37 °C (123%, P = 0.013), which was blocked by congo red in a concentration-dependent manner (59−33% in 1−10 μM, P = 0.003−0.000). Nevertheless, no inhibitory potency was observed with indole and NC001-8 (121−127%, P = 0.363−0.897), suggesting that the mechanism of reducing ATXN3/Q_{75} aggregation on cells was not through direct interference with ATXN3/Q_{75} aggregate formation.

dx.doi.org/10.1021/cn500075u | ACS Chem. Neurosci. 2014, 5, 1063−1074

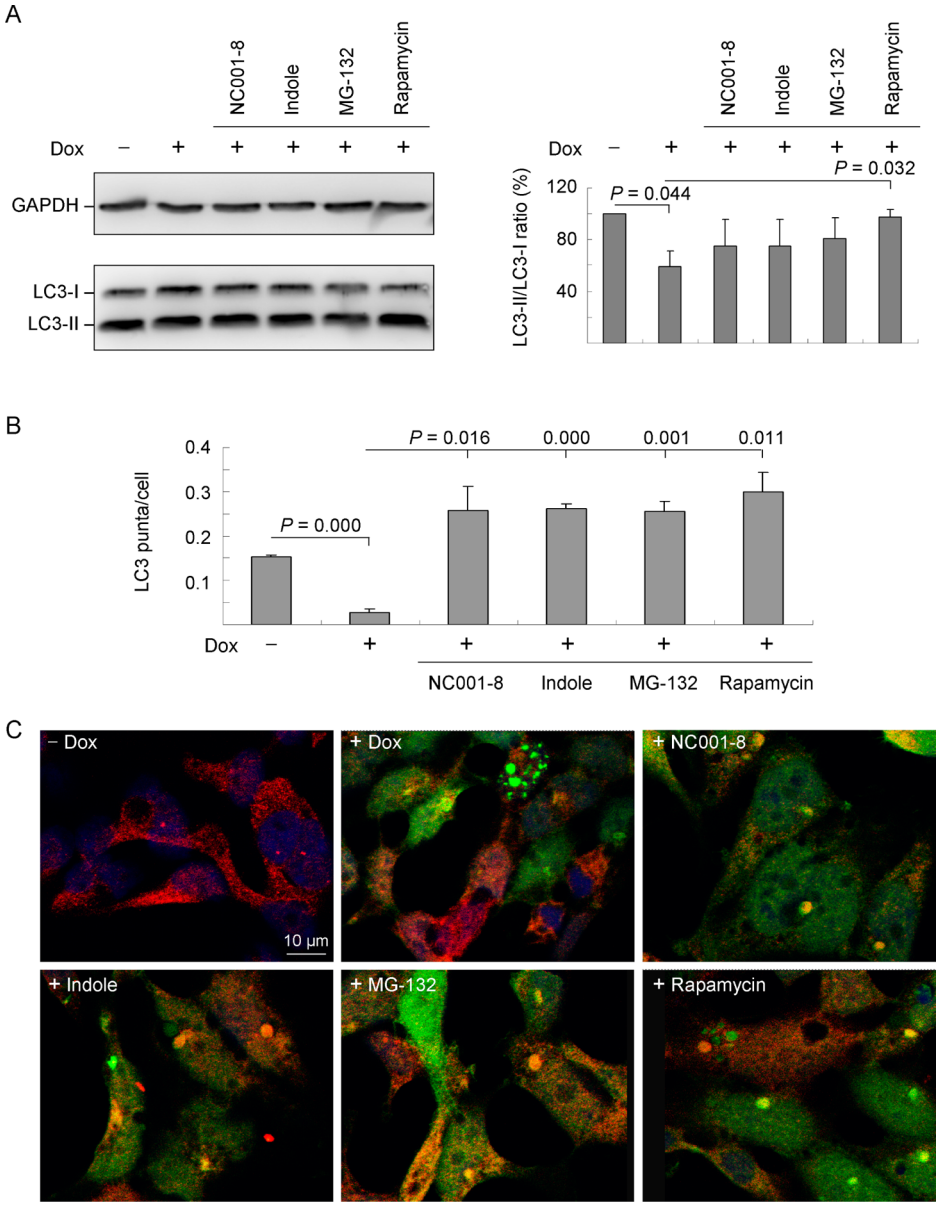

Figure 7. Indole and NC001-8 enhanced autophagy in ATXN3/Q_{75} expressing cells. (A) ATXN3/Q_{75} 293 cells were untreated or pretreated with indole, NC001-8, MG-132 (0.1 μM), or rapamycin (0.2 μM) for 8 h and ATXN3/Q_{75}-GFP expression induced for 6 days. Relative LC3-I and LC3-II were analyzed by Western blot analysis using LC3 and GAPDH (as a loading control) antibodies. Data are expressed as the mean ± SD values from three independent experiments. (B) LC3 punta in the above 293 cells with indole/NC001-8/MG-132/rapamycin pretreatment and ATXN3/Q_{75}-GFP induced expression for 6 days were assessed by HCA system. (C) Typical morphological changes of autophagosome in ATXN3/Q_{75}-GFP cells pretreated with indole, NC001-8, MG-132 (0.1 μM), and rapamycin (0.2 μM) (blue, nuclei; green, expressed ATXN3/Q_{75}-GFP protein; red, LC3).

Indole Compounds Enhance Chaperone Expression on 293 Cells. Because indole compound indomethacin was reported to induce the expression of heat shock proteins,[22] 293 cells with mCherry, AmCyan1, and ZsYellow1 fluorescent reporters downstream of HSF1, HSPA1A, and HSPA8 promoters[24] were used to test the potential of indole/NC001-8 to enhance HSF1 and HSP70 chaperone expression. As shown in Figure 4, treatment with GGA (0.1−1 μM) for 1 day significantly increased HSF1 (110%, P = 0.035−0.009), HSPA1A (112%, P = 0.020−0.013), and HSPA8 (108−110%, P = 0.030−0.020) promoter activity. This was also true for indole and NC001-8 treatments (0.1−1 μM), with 110−115% HSF1 (P = 0.030−0.016), 112−115% HSPA1A (P = 0.039−0.008) and 109−110% HSPA8 (P = 0.012−0.001) promoter activities compared with no treatment (100%). This finding suggested that indole and NC001-8 enhanced chaperone expression on 293 cells.

Indole Compounds Enhance Autophagy on 293 Cells. Previously a phenylindole derivative, sertindole, was reported to induce autophagy in SH-SY5Y neuroblastoma cells.[29] To test indole and NC001-8 potential to enhance autophagy activity, we established a 293-based fluorescent reporter cell model with induced DsRed-LC3 expression. As shown in Figure 5A, the LC3 antibody detected a 42 kDa DsRed-LC3 protein after 2 days induction with doxycycline (+ Dox). After induction of DsRed-LC3 expression for 1 day, cells were treated with rapamycin (0.2 μM),[30] indole, or NC001-8 (0.1−1.0 μM) for 24 h. DsRed-LC3-positive vacuoles (punta) were quantified as

dx.doi.org/10.1021/cn500075u | ACS Chem. Neurosci. 2014, 5, 1063−1074

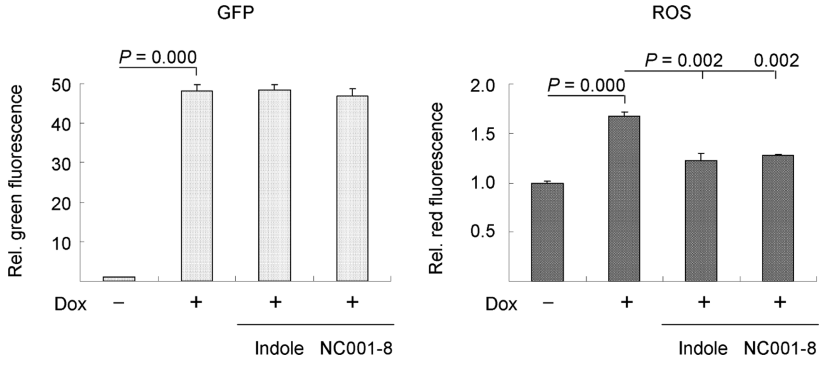

Figure 8. Prevention of the induction of ROS by indole and NC001-8 in ATXN3/Q_{75}-GFP 293 cells. Cells were pretreated with indole and NC001-8 (0.1 μM) for 8 h, and ATXN3/Q_{75}-GFP expression was induced for 6 days. The induced ATXN3/Q_{75}-GFP (green fluorescence) and reactive oxygen species (ROS) detected by CellROX reagent (red fluorescence) were measured. Each represented the means ± SD of three separate experiments.

indicative of autophagosome formation. As shown in Figure 5B, treatment of rapamycin significantly induced the recruitment of DsRed-LC3 to autophagic vacuoles (127%, P = 0.038). This was also true for indole and NC001-8 treatments, with 113−127% punta for indole (P = 0.029−0.004) and 112−126% punta for NC001-8 (P = 0.044−0.041) treatment compared with no treatment (100%). This finding suggested that indole and NC001-8 enhanced autophagy activity on 293 cells.

Indole Compounds Enhance Chaperone Expression on 293 ATXN3/Q_{75} Cells, and HSPA1A Overexpression Reduces ATXN3/Q_{75} Aggregation. To examine whether indole and NC001-8 up-regulated HSF1 and chaperone expression in ATXN3/Q_{75} 293 cells, we compared the expression levels of HSF1, HSPA8, and HSPA1A with and without indole or NC001-8 and Dox treatment. As shown in Figure 6A, induced expression of ATXN3/Q_{75} (+ Dox) for 6 days attenuated the expression of HSF1 (85%, P = 0.008), HSPA8 (86%, P = 0.019), and HSPA1A (86%, P = 0.043) compared with uninduced cells (100%). This reduction can be rescued by the addition of GGA, indole, or NC001-8 (0.1 μM), with significantly increased HSF1 (105−115%, P = 0.030−0.011), HSPA8 (109−118%, P = 0.041−0.009), and HSPA1A (104−110%, P = 0.048−0.013) expression compared with untreated cells (85−86%). These findings indicated that in addition to GGA, indole and NC001-8 up-regulated HSF1, HSPA8, and HSPA1A expression to reduce ATXN3/Q_{75} aggregation in cell model.

To determine whether HSPA1A could suppress aggregation of mutant ATXN3, we transiently coexpressed HSPA1A with ATXN3/Q_{75} in HEK-293T cells. As shown in Figure 6B, with similar ATXN3/Q_{75} expression level (99.9%) and increased HSPA1A expression level (164.6%), visible aggregates significantly decreased in ATXN3/Q_{75} cells cotransfected with HSPA1A compared with cells cotransfected with vector only (10.4% vs 14.8%, P = 0.010). The extent of polyQ aggregate reduction in ATXN3/Q_{75} and HSPA1A cotransfected cells (10.4%/14.8%=70%) is less than that with indole compound treatment (Figure 2C, 70−84%), because indole compounds also induce autophagy. The results of reducing ATXN3/Q_{75} aggregation through enhancing cellular chaperone expression suggest the therapeutic potentials of indole and its synthetic derivative NC001-8 for SCA.

In polyQ-mediated SCA, the inclusion of the disease-causing proteins affects the molecular chaperone pathway.[31] Our previous studies also showed that decreased heat shock cognate HSPA8 protein (a constitutive HSP70) expression could underlie pathogenesis of SCA17.[32,33] HSP70 has been reported to suppress polyQ-mediated neurodegeneration in *Drosophila*.[34] Overexpression of heat-inducible HSP70 chaperone (HSPA1A) suppresses neuropathology and improves motor function in SCA1 mice.[35] Expression of molecular chaperones is regulated by HSF1, and HSF1-activating compounds have been indicated as therapeutic candidates for polyQ disorders.[36,37] Our results of neuroprotection via enhancement of the chaperone system provide a novel mechanism of indole and derivative NC001-8 to decelerate the neurodegenerative process.

Indole Compounds Enhance Autophagy Activity on 293 ATXN3/Q_{75} Cells. To examine whether indole and NC001-8 also induced autophagy in ATXN3/Q_{75} 293 cells, we first compared the expression levels of lipid phosphatidylethanolamine (PE)-conjugated LC3-II and cytosolic LC3-I in cells with and without indole or NC001-8 and Dox treatment, because LC3-II is the only known protein that specifically associates with autophagosomes and not with other vesicular structures.[38] As shown in Figure 7A, induced expression of ATXN3/Q_{75} (+ Dox) for 6 days attenuated the LC3-II/LC3-I ratio (59%, P = 0.044) compared with uninduced cells (100%). A significantly increased LC3-II/LC3-I ratio compared with untreated cells (98% vs 59%, P = 0.032) was observed with the addition of rapamycin (0.2 μM). The rescue of reduction was also notable (75−81% vs 59%) with the addition of indole, NC001-8, and MG-132 (0.1 μM).[39] MG-132, an inhibitor of proteasome, may activate chaperone-mediated autophagy (CMA) like the reported proteasome inhibitor epoxomicin.[40] We then quantified punta in these ATXN3/Q_{75} 293 cells. As shown in Figure 7B, induced expression of ATXN3/Q_{75} significantly reduced punta number per cell (0.03 vs 0.15, P = 0.000). Treatment of NC001-8, indole, MG-132, and rapamycin significantly induced the recruitment of DsRed-LC3 to autophagic vacuole (0.26−0.30 vs 0.03, P = 0.016−0.000). Representative fluorescence microscopy images in uninduced cells, untreated cells, and after treatment with NC001-8, indole, MG-132, and rapamycin are shown in Figure 7C. The colocalization of polyQ aggregates (green) with LC3 (red) in indole compounds, MG-132, and rapamycin treated cells also supports the notion of polyQ aggregate reduction by autophagy. Thus, in ATXN3/Q_{75}-GFP expressing cells pretreated with indole and NC001-8, the increased appearance of LC3 fluorescent punta and reduced appearance of ATXN3/Q_{75}

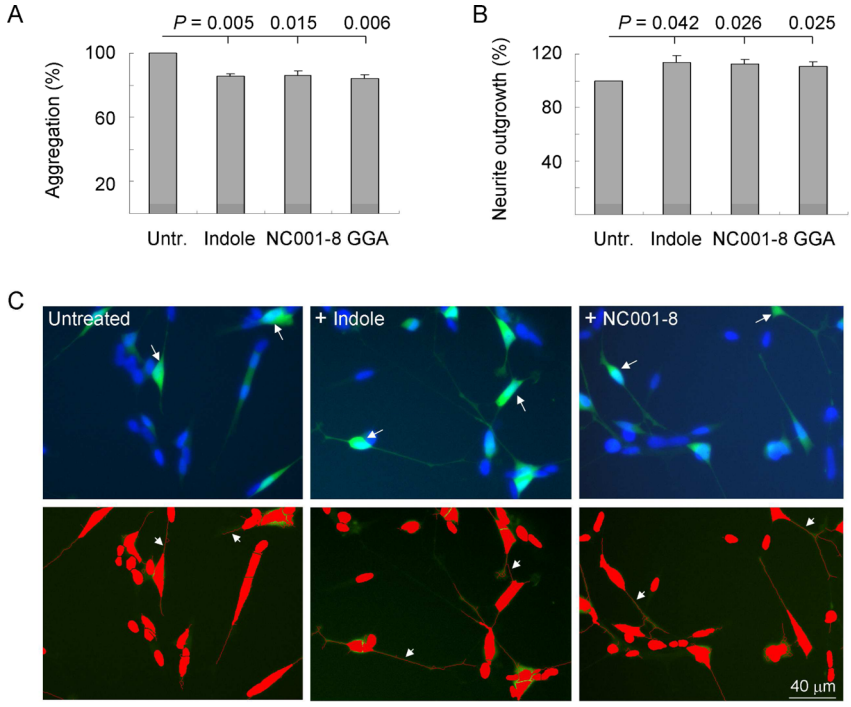

Figure 9. Reduction of aggregation and promotion of neurite outgrowth of ATXN3/Q_{75} SH-SY5Y cells by indole and NC001-8. (A) Relative aggregation after treatment with indole, NC001-8, and GGA (0.1 μM) for 1 week. To normalize, the relative aggregation level in untreated cells is set as 100%. (B) Relative neurite outgrowth after indole/NC001-8/GGA treatment (0.1 μM). To normalize, the outgrowth level in untreated cells is set as 100%. (C) Representative microscopic images of differentiated ATXN3/Q_{75}-GFP SH-SY5Y cells untreated or treated with indole/NC001-8 (0.1 μM) for 6 days (blue, nuclei; green, expressed ATXN3/Q_{75}-GFP protein; red, cell body and outgrowth segmentation). Arrows indicate polyQ aggregate expressed SH-SY5Y cells; arrow-heads indicate outgrowth neurite.

aggregates indicated that indole and NC001-8 enhanced autophagy activity on 293 ATXN3/Q_{75} cell model.

The autophagy–lysosomal system regulates protein degradation for maintaining cellular homeostasis. Autophagy has been proposed as a strategy to reduce the accumulation of expanded-polyQ aggregates and protect against mutant protein neurotoxicity.[41] Pharmacological augmentation of autophagy using rapamycin resulted in accelerated turnover of expanded polyQ protein and reduced neurodegeneration in cell and animal models of polyQ disease.[42] Administration of temsirolimus (a rapamycin ester) improved motor performance in SCA3 transgenic mouse model by reducing the number of mutant ataxin-3 aggregates by autophagy.[43] Our results that treatment with indole and NC001-8 led to the enhancement of autophagy activity consolidate the role of indole and NC001-8 in aggregation reduction for SCA treatment.

Indole Compounds Reduce ROS Production on 293 ATXN3/Q_{75} Cells. To evaluate whether indole and NC001-8 reduced ROS formation in 293 ATXN3/Q_{75} cells, the cellular production of ROS was measured by using a red fluorescent probe from Molecular Probes. As shown in Figure 8, induced expression of ATXN3/Q_{75} (+ Dox) for 6 days significantly increased ROS production (168%, P = 0.000) compared with uninduced cells (100%). With similarly induced green fluorescence (46.8–48.4-fold, P = 0.295–0.858), indole and NC001-8 significantly ameliorated oxidative stress induced by ATXN3/Q_{75} compared with untreated cells (red fluorescence from 168% to 123–128%, P = 0.002). Previously, endogenous IPAM was also reported to act as a stabilizer of energy metabolism thereby reducing ROS production.[20] It has been proven that the presence of polyQ mutation induces ROS to increase oxidative stress.[44] Our data that indole and its synthetic derivative NC001-8 decreased ROS and displayed neuroprotective effects were in agreement with these reports.

During oxidative stress, CMA is activated to selectively degrade cytosolic proteins in lysosomes.[45] It has been shown that CMA enhancement facilitated degradation of mutant protein in a HD animal model.[46] Because expanded ATXN3/Q_{75} induced ROS in ATXN3/Q_{75} cells, the observed autophagy activation by indole and NC001-8 may also be mediated by CMA. Examination of autophagy with chaperone knockdown may help to establish the connection of chaperone and autophage in aggregation reduction by indole and NC001-8.

Indole Compounds Promote Neurite Outgrowth on ATXN3/Q_{75} SH-SY5Y Cells. To test the neurite outgrowth-promoting potential of indole and NC001-8, we constructed SH-SY5Y cells with N-terminally truncated ATXN3/Q_{75}-GFP expression in an inducible fashion.[24] The ATXN3/Q_{75}-GFP SH-SY5Y cells can be differentiated using retinoic acid.[47,48] After 1 week of neuronal differentiation, the induced ATXN3/Q_{75}-GFP formed aggregates in ~1% of differentiated neurons.[49] The treatments with indole, NC001-8, and GGA led to 14–16% aggregation reduction (P = 0.015–0.005) in ATXN3/Q_{75}-expressing neuronal cells (Figure 9A), accompanying increased total outgrowth (111–114%, P = 0.042–0.025; Figure 9B). Representative fluorescence microscopy images after treatment with indole and NC001-8 are shown in Figure 9C. These results confirmed the aggregation-inhibitory and neurite outgrowth-promoting effects of indole, NC001-8, and GGA in differentiated neurons.

■ CONCLUSION

The experiments above provide strong evidence that indole and NC001-8 could be novel therapeutics for SCA3 and other

polyQ diseases. Despite compelling evidence for the potent antiaggregation properties of indole and NC001-8, the direct cellular target(s) have not been uncovered. Indole and NC001-8 appear to affect important cellular pathways that regulate the fate of aggregating proteins (e.g., autophagy and chaperone induction) but do not directly affect aggregation. Because indole is the precursor to many pharmaceuticals and indole and its derivatives can be synthesized by a variety of methods,[50,51] development of indole-based compounds offers a promising strategy for the treatment of polyQ diseases. Future computational analysis is warranted to achieve a clear structure−activity relationship of these indole compounds. Investigations of indole and NC001-8 in more SCA or other polyQ disease animal models would solidify their effects on aggregation reduction and disease improvement. Since the pathogenesis of the polyQ diseases is not completely clear and effective treatment is not available, our SCA disease model systems described in this study could be potential platforms for evaluating more promising treatment for polyQ diseases. A systemic high-throughput screening of herbal and chemical compounds using ATXN3/Q_{75} 293 cells is underway.

METHODS

Cell Culture and Cell Proliferation Assay. Human embryonic kidney 293 cells (ATCC No. CRL-1573) were cultivated in Dulbecco's modified Eagle's medium (DMEM) containing 10% fetal bovine serum (FBS) (Invitrogen). Cells were cultivated in a 37 °C incubator containing 5% CO_2, and cell proliferation was measured based upon the reduction of 3-[4,5-dimethylthiazol-2-yl]-2,5-diphenyltetrazolium bromide (MTT). Briefly, 5×10^4 cells were plated into 48-well dishes, grown for 20 h, and treated with 0.1−10 μM indole and derivatives.[23] After 1 day, 20 μL of MTT (5 mg/mL in PBS, Sigma) was added to cells and incubated for 2 h. The absorbance of the insoluble purple formazan product was measured at 570 nm by a Bio-Tek μQuant Universal microplate spectrophotometer.

ATXN3 cDNA Constructs and Flp-In 293 ATXN3 Cell Lines. The cloning of plasmids containing GFP-tagged ATXN3 C-terminal Q_{14-75}-containing fragment and the establishment of Flp-In 293 cells with ATXN3-GFP expression in an inducible fashion were as described.[24] The recombinant ATXN3/Q_{14-75}-GFP is under the control of a tetracycline-regulated hybrid human cytomegalovirus (CMV)/$TetO_2$ promoter, which can be induced by the addition of doxycycline. The repeats in these ATXN3 cell lines were examined by PCR and sequencing. These cell lines were grown in medium containing 5 μg/mL blasticidin and 100 μg/mL hygromycin (InvivoGen).

ATXN3/Q_{75} Aggregation Assay. ATXN3/Q_{75}-GFP 293 cells were plated into 96-well (2×10^4/well) dishes, grown for 24 h, and treated with different concentrations of the GGA or indole compounds (0.1−1 μM) for 8 h. Then doxycycline (10 μg/mL) and oxaliplatin (5 μM, Sigma) were added for 6 days. Oxaliplatin was added for aggregate accumulation through inhibition of cell division.[52] After that, cells were stained with Hoechst 33342 (0.1 μg/mL, Sigma), and images of the cells were automatically obtained using MetaXpress Image Acquisition and Analysis Software (Molecular Devices), with excitation/emission wavelengths at 482/536 (EGFP). Aggregation was determined by Transfluor technology[26] based on GFP intensity.

Trx- and His-Tagged ATXN3/Q_{14-75} and Thioflavin T Binding Assay. PCR was performed using the cloned ATXN3/Q_{14-75}-GFP as templates and synthetic primers 5′-GCATGCAAGGTAGTTCCAGAAAC (*Nla*III site underlined) and 5′-CATGCCATGGCATGTTTTTTTCCTTCTGTT (*Nco*I site underlined). The amplified polyQ-containing cDNA fragments were cloned into pGEM-T Easy (Promega) and sequenced. The ATXN3/Q_{14-75} cDNAs were excised with *Nla*III and *Nco*I and subcloned into *Nla*III- and *Nco*I-digested pET-32b(+) (Novagen). The resulting plasmids were transformed into BL21(DE3)pLysS (Novagen) and Trx (thioredoxin)- and His-tagged ATXN3/Q_{14-75} protein expression was induced with 0.1 mM isopropyl-β-D-thiogalactopyranoside (IPTG) for 3 h at 25 °C. Bacterial cells were then harvested, and the Trx-His-ATXN3/Q_{14-75} proteins were purified using His-Bind resins (Novagen) according to supplier's instructions.

For thioflavin T binding assay, ATXN3 protein (2.5 μM final concentration) was incubated with tested compounds (congo red, indole, and NC001-8; 0.1−10 μM) in 150 mM NaCl and 20 mM Tris-HCl, pH 8.0, at 37 °C for 48 h to form aggregates. Then thioflavin T (20 μM final concentration; Sigma) was added and incubated for 15 min at room temperature. Thioflavin T fluorescence intensity of samples was recorded by using a microplate reader (Bio-Tek FLx800), with excitation 420 nm and emission 485 nm filter combination.

Triple Fluorescent Reporter Cells and Fluorescent Assay. The Flp-In triple fluorescent reporter cells were maintained as described.[24] GGA (Cayman Chemical), indole, or NC001-8 (0.1−1 μM) was added to the medium for 24 h. The three fluorescence colors were analyzed simultaneously using high-content analysis (HCA) system (ImageXpressMICRO, Molecular Devices), with excitation/emission wavelengths at 453/486 (mCherry), 587/610 (AmCyan1), and 531/540 nm (ZsYellow1).

DsRed-LC3 Cells and Autophagy Assay. The pDsRed-LC3 construct encoding human microtubule-associated protein 1 light chain 3β (MAP1LC3B, NM_022818) was generated by PCR amplification of LC3 coding sequence from human cDNA using the forward (5′-AAGCTTCCATGCCGTCGGAGAAG, *Hin*dIII site underlined) and reverse (5′-TTTTACACTGACAATTTCATC) primers. The amplified LC3 cDNA was cloned into pGEM-T Easy (Promega) and sequenced. The LC3 cDNA was excised with *Hin*dIII and *Eco*RI (in pGEM-T Easy) restriction enzymes and subcloned into the corresponding sites of pDsRed-Monomer-C1 (Clontech). Then the *Age*I (blunted)−*Bam*HI (in pDsRed-Monomer-C1) DNA fragment containing in-frame DsRed-LC3 was ligated with *Bam*HI−*Ahd*I (997−4215) and *Ahd*I−*Eco*RV (4215−1032) fragments of pcDNA5/FRT/TO (Invitrogen). The Flp-In DsRed-LC3 cells were generated using the resulting plasmid according to the supplier's instructions (Invitrogen) and maintained in medium containing 5 μg/mL blasticidin and 100 μg/mL hygromycin.

For examining autophagy activity induced by indole and NC001-8, DsRed-LC3 cells were plated into 96-well (2×10^4/well) dishes. The next day, doxycycline (1 μg/mL, BD) was added to induce DsRed-LC3 expression. Then rapamycin (0.2 μM), indole, or NC001-8 (0.1−1 μM) was added to the medium for 1 day, and punta within cells was analyzed at 562/624 nm using HCA. Punta was determined by Transfluor technology[26] based on DsRed intensity.

Caspase Activity Assay. Caspase 3 activity was measured with the Caspase 3 assay kit according to the manufacturer's instructions (Sigma). Briefly, cells (10^6) were incubated with lysis buffer (100 μL) on ice for 20 min. After centrifugation, proteins in supernatants were quantified, and caspase 3 activity was measured using acetyl-Asp-Glu-Val-Asp-7-amido-4-methylcoumarin (Ac-DEVD-AMC) as substrate. The release of the fluorescent AMC was recorded in an FLx800 microplate fluorescence reader (Bio-Tek) at 360 nm excitation filter in conjunction with 460 nm emission filter. The caspase 3 activity was calculated using an AMC standard curve.

Western Blot Analysis. Total proteins were prepared using lysis buffer containing 5% glycerol, 0.5% Triton X-100, 1 mM dithiothreitol, and protease inhibitor cocktail (Sigma). Proteins (20 μg) were separated on 10% SDS-polyacrylamide gel electrophoresis and blotted on to nitrocellulose membranes by reverse electrophoresis. After blocking, the membrane was probed with HSF1 (1:1000 dilution, Abnova), HSPA8 (1:500 dilution, Santa Cruz), HSPA1A (1:500 dilution, Santa Cruz), GFP (1:500 dilution, Santa Cruz), LC3 (1:3000 dilution, MBL International), β-actin (1:5000 dilution, Millipore), or GAPDH (1:1000 dilution, MDBio) at 4 °C overnight. Then the immune complexes were detected by horseradish peroxidase-conjugated goat anti-mouse or goat anti-rabbit IgG antibody (1:5000 dilution, GeneTex) and chemiluminescent substrate (Millipore).

ATXN3/Q_{75} and HSPA1A cDNA Cotransfection. The HSPA1A cDNA (BC002453) in pOTB7 was obtained from Bioresource

Collection and Research Center (BCRC), Food Industry Research and Development Institute, Taiwan. The cDNA was excised with *Eco*RI and *Xho*I and subcloned into pcDNA3 (Invitrogen). Human embryonic kidney HEK-293T cells (ATCC No. CRL-11268) were cultivated in DMEM containing 10% FBS as described. For transient overexpression, cells were plated into 12-well (1×10^5/well) dishes, grown for 20 h, and transfected using T-Pro reagent with pcDNA5/FRT/TO-ATXN3/Q_{75} and pcDNA3-HSPA1A or pcDNA3 vector plasmids (1.5 μg each). The cells were grown for 48 h for ATXN3/Q_{75} aggregation assay as described.

Reactive Oxygen Species (ROS) Analysis. ATXN3/Q_{75}-GFP 293 cells were plated into six-well (10^5/well) dishes, treated with indole or NC001-8 for 8 h, and induced for ATXN3/Q_{75}-GFP expression for 6 days as described above for aggregate accumulation. Then fluorogenic CellROX deep red reagent (5 μM, Molecular Probes) was added to the cells and incubated at 37 °C for 30 min. For measuring ROS, cells were analyzed for green (GFP) and red (ROS) fluorescence on a flow cytometry system (Becton−Dickinson), with excitation/emission wavelengths at 488/507 (green) and 640/665 nm (red).

Immunocytochemical Staining of ATXN3/Q_{75} Cells. ATXN3/Q_{75} cells on coverslips were washed with PBS and fixed in 4% paraformaldehyde at room temperature for 30 min. After washing twice with PBS, cells were permeabilized at room temperature for 10 min with 0.1% Triton X-100 and then blocked with 3% bovine serum albumin (BSA) for 2 h at room temperature. The primary anti-LC3 antibody (1:100 dilution) was used to stain cells at 4 °C overnight, and cells were washed three times with PBS containing 0.1% Tween 20 (PBST). After washing, cells were incubated for 2 h at room temperature in TRITC-conjugated secondary antibody (1:500 dilution, Zymed) and washed three times with PBST. Nuclei were detected using 4′-6-diamidino-2-phenylindole (DAPI). The stained cells were examined after being mounted in Vectashield (Vector Laboratories Inc.) using a Leica TCS confocal laser scanning microscope. LC3 punta and total cell number of three randomly selected fields were counted.

SH-SY5Y ATXN3/Q_{75} Cells Aggregation and Neurite Outgrowth Assays. The Flp-In SH-SY5Y ATXN3/Q_{75} cells were established as described.[24] Cells were seeded in 6-well (2×10^5/well) plates, with all *trans*-retinoic acid (10 μM, Sigma) added at seeding time. At day 2, cells were treated with indole, NC001-8, or GGA (0.1 μM) for 8 h, and then doxycycline (5 μg/mL) was added to induce ATXN3/Q_{75}-GFP expression. The cells were kept in the medium containing 10 μM *trans*-retinoic acid, doxycycline, and indole/NC001-8/GGA for 6 days. After that, cells were stained with Hoechst 33342 (0.1 μg/mL), and aggregation percentage was assessed as described. The total neurite outgrowth of untreated and indole/NC001-8/GGA-treated cells was assessed by using Metamorph microscopy automation and image analysis software (neurite outgrowth application module, Molecular Devices).

Statistical Analysis. For each set of values, data were expressed as the means ± standard deviation (SD). Three independent experiments were performed and noncategorical variables were compared using the Student's *t*-test. All *P*-values were two-tailed, with values of $P < 0.05$ considered significant.

AUTHOR INFORMATION

Corresponding Authors

*E-mail: t43019@ntnu.edu.tw (G.-J.L.-C.).
*E-mail: cheyaocf@ntnu.edu.tw (C.F.Y.).

Author Contributions

C.-H. Lin and Y.-R. Wu contributed equally to this work.

Funding

This work was funded by the Grants NSC102-2325-B-003-002, NSC102-2811-B-182A-013, and NSC102-2314-B-182A-113-MY2 from the National Science Council, Executive Yuan, and 103T3040B05 from National Taiwan Normal University, Taipei, Taiwan.

Notes

The authors declare no competing financial interest.

ACKNOWLEDGMENTS

The authors thank the Molecular Imaging Core Facility of National Taiwan Normal University for the technical assistance.

REFERENCES

(1) Orr, H. T., Chung, M. Y., Banfi, S., Kwiatkowski, T. J., Jr., Servadio, A., Beaudet, A. L., McCall, A. E., Duvick, L. A., Ranum, L. P., and Zoghbi, H. Y. (1993) Expansion of an unstable trinucleotide CAG repeat in spinocerebellar ataxia type I. *Nat. Genet. 4*, 211−226.

(2) Pulst, S. M., Nechiporuk, A., Nechiporuk, T., Gispert, S., Chen, X. N., Lopes-Cendes, I., Pearlman, S., Starkman, S., Orozco-Diaz, G., Lunkes, A., DeJong, P., Rouleau, G. A., Auburger, G., Korenberg, J. R., Figueroa, C., and Sahba, S. (1996) Moderate expansion of a normally biallelic trinucleotide repeat in spinocerebellar ataxia type 2. *Nat. Genet. 14*, 269−276.

(3) Kawaguchi, Y., Okamoto, T., Taniwaki, M., Aizawa, M., Inoue, M., Katayama, S., Kawakami, H., Nakamura, S., Nishimura, M., Akiguchi, I., Kimura, J., Narumiya, S., and Kakizuka, A. (1996) CAG expansions in a novel gene for Machado−Joseph disease at chromosome 14q32.1. *Nat. Genet. 8*, 221−228.

(4) Zhuchenko, O., Bailey, J., Bonnen, P., Ashizawa, T., Stockton, D. W., Amos, C., Dobyns, W. B., Subramony, S. H., Zoghbi, H. Y., and Lee, C. C. (1997) Autosomal dominant cerebellar ataxia (SCA6) associated with small polyglutamine expansions in the α_{1A}-voltage-dependent calcium channel. *Nat. Genet. 15*, 62−69.

(5) David, G., Abbas, N., Stevanin, G., Dürr, A., Yvert, G., Cancel, G., Weber, C., Imbert, G., Saudou, F., Antoniou, E., Drabkin, H., Gemmill, R., Giunti, P., Benomar, A., Wood, N., Ruberg, M., Agid, Y., Mandel, J. L., and Brice, A. (1997) Cloning of the SCA7 gene reveals a highly unstable CAG repeat expansion. *Nat. Genet. 17*, 65−70.

(6) Moseley, M. L., Zu, T., Ikeda, Y., Gao, W., Mosemiller, A. K., Daughters, R. S., Chen, G., Weatherspoon, M. R., Clark, H. B., Ebner, T. J., Day, J. W., and Ranum, L. P. (2006) Bidirectional expression of CUG and CAG expansion transcripts and intranuclear polyglutamine inclusions in spinocerebellar ataxia type 8. *Nat. Genet. 38*, 758−769.

(7) Koide, R., Kobayashi, S., Shimohata, T., Ikeuchi, T., Maruyama, M., Saito, M., Yamada, M., Takahashi, H., and Tsuji, S. (1999) A neurological disease caused by an expanded CAG trinucleotide repeat in the TATA-binding protein gene: a new polyglutamine disease? *Hum. Mol. Genet. 8*, 2047−2053.

(8) Koide, R., Ikeuchi, T., Onodera, O., Tanaka, H., Igarashi, S., Endo, K., Takahashi, H., Kondo, R., Ishikawa, A., Hayashi, T., Saito, M., Tomoda, A., Miike, T., Naito, H., Ikuta, F., and Tsuji, S. (1994) Unstable expansion of CAG repeat in hereditary dentatorubral-pallidoluysian atrophy (DRPLA). *Nat. Genet. 6*, 9−13.

(9) Zoghbi, H. Y., and Orr, H. T. (1999) Polyglutamine diseases: Protein cleavage and aggregation. *Curr. Opin. Neurobiol. 9*, 566−570.

(10) Gatchel, J. R., and Zoghbi, H. Y. (2005) Diseases of unstable repeat expansion: Mechanisms and common principles. *Nat. Rev. Genet. 6*, 743−755.

(11) Schols, L., Bauer, P., Schmidt, T., Schulte, T., and Riess, O. (2004) Autosomal dominant cerebellar ataxias: Clinical features, genetics, and pathogenesis. *Lancet Neurol. 3*, 291−304.

(12) Soong, B. W., Lu, Y. C., Choo, K. B., and Lee, H. Y. (2001) Frequency analysis of autosomal dominant cerebellar ataxias in Taiwanese patients and clinical and molecular characterization of spinocerebellar ataxia type 6. *Arch. Neurol. 58*, 1105−1109.

(13) Wu, Y. R., Lin, H. Y., Chen, C. M., Gwinn-Hardy, K., Ro, L. S., Wang, Y. C., Li, S. H., Hwang, J. C., Fang, K., Hsieh-Li, H. M., Li, M. L., Tung, L. C., Su, M. T., Lu, K. T., and Lee-Chen, G. J. (2004) Genetic testing in spinocerebellar ataxia in Taiwan: Expansions of trinucleotide repeats in SCA8 and SCA17 are associated with typical Parkinson's disease. *Clin. Genet. 65*, 209−214.

(14) Haacke, A., Broadley, S. A., Boteva, R., Tzvetkov, N., Hartl, F. U., and Breuer, P. (2006) Proteolytic cleavage of polyglutamine-

expanded ataxin-3 is critical for aggregation and sequestration of non-expanded ataxin-3. *Hum. Mol. Genet. 15*, 555−568.
(15) Ahmad, A., Biersack, B., Li, Y., Kong, D., Bao, B., Schobert, R., Padhye, S. B., and Sarkar, F. H. (2013) Targeted regulation of PI3K/Akt/mTOR/NF-κB signaling by indole compounds and their derivatives: mechanistic details and biological implications for cancer therapy. *Anticancer Agents Med. Chem. 13*, 1002−1013.
(16) Biersack, B., and Schobert, R. (2012) Indole compounds against breast cancer: Recent developments. *Curr. Drug Targets 13*, 1705−1719.
(17) Aggarwal, B. B., and Ichikawa, H. (2005) Molecular targets and anticancer potential of indole-3-carbinol and its derivatives. *Cell Cycle 4*, 1201−1215.
(18) Rogan, E. G. (2006) The natural chemopreventive compound indole-3-carbinol: State of the science. *In Vivo 20*, 221−228.
(19) Chyan, Y. J., Poeggeler, B., Omar, R. A., Chain, D. G., Frangione, B., Ghiso, J., and Pappolla, M. A. (1999) Potent neuroprotective properties against the Alzheimer β-amyloid by an endogenous melatonin-related indole structure, indole-3-propionic acid. *J. Biol. Chem. 274*, 21937−21942.
(20) Poeggeler, B., Sambamurti, K., Siedlak, S. L., Perry, G., Smith, M. A., and Pappolla, M. A. (2010) A novel endogenous indole protects rodent mitochondria and extends rotifer lifespan. *PLoS One 5*, No. e10206.
(21) Lee, C. H., Yao, C. F., Huang, S. M., Ko, S., Tan, Y. H., Lee-Chen, G. J., and Wang, Y. C. (2008) Novel 2-step synthetic indole compound 1,1,3-tri(3-indolyl)cyclohexane inhibits cancer cell growth in lung cancer cells and xenograft models. *Cancer 113*, 815−825.
(22) Ishihara, K., Yamagishi, N., and Hatayama, T. (2004) Suppression of heat- and polyglutamine-induced cytotoxicity by nonsteroidal anti-inflammatory drugs. *Eur. J. Biochem. 271*, 4552−4558.
(23) Janreddy, D., Kavala, V., Bosco, J. W. J., Kuo, C. W., and Yao, C. F. (2011) An easy access to carbazolones and 2,3-disubstituted indoles. *Eur. J. Org. Chem. 12*, 2360−2365.
(24) Chang, K. H., Chen, W. L., Lee, L. C., Lin, C. H., Kung, P. J., Lin, T. H., Wu, Y. C., Wu, Y. R., Chen, Y. C., Lee-Chen, G. J., and Chen, C. M. (2013) Aqueous extract of *Paeonia lactiflora* and paeoniflorin as aggregation reducers targeting chaperones in cell models of spinocerebellar ataxia 3. *Evidence-Based Complementary Altern. Med. 2013*, No. 471659.
(25) Yamanaka, K., Takahashi, N., Ooie, T., Kaneda, K., Yoshimatsu, H., and Saikawa, T. (2003) Role of protein kinase C in geranylgeranylacetone-induced expression of heat-shock protein 72 and cardioprotection in the rat heart. *J. Mol. Cell. Cardiol. 35*, 785−794.
(26) Ghosh, R. N., DeBiasio, R., Hudson, C. C., Ramer, E. R., Cowan, C. L., and Oakley, R. H. (2005) Quantitative cell-based high-content screening for vasopressin receptor agonists using transfluor technology. *J. Biomol. Screening 10*, 476−484.
(27) Endo, S., Hiramatsu, N., Hayakawa, K., Okamura, M., Kasai, A., Tagawa, Y., Sawada, N., Yao, J., and Kitamura, M. (2007) Geranylgeranylacetone, an inducer of the 70-kDa heat shock protein (HSP70), elicits unfolded protein response and coordinates cellular fate independently of HSP70. *Mol. Pharmacol. 72*, 1337−1348.
(28) Heiser, V., Scherzinger, E., Boeddrich, A., Nordhoff, E., Lurz, R., Schugardt, N., Lehrach, H., and Wanker, E. E. (2000) Inhibition of huntingtin fibrillogenesis by specific antibodies and small molecules: implications for Huntington's disease therapy. *Proc. Natl. Acad. Sci. U. S. A. 97*, 6739−6744.
(29) Shin, J. H., Park, S. J., Kim, E. S., Jo, Y. K., Hong, J., and Cho, D. H. (2012) Sertindole, a potent antagonist at dopamine D_2 receptors, induces autophagy by increasing reactive oxygen species in SH-SY5Y neuroblastoma cells. *Biol. Pharm. Bull. 35*, 1069−1075.
(30) Berger, Z., Ravikumar, B., Menzies, F. M., Oroz, L. G., Underwood, B. R., Pangalos, M. N., Schmitt, I., Wullner, U., Evert, B. O., O'Kane, C. J., and Rubinsztein, D. C. (2006) Rapamycin alleviates toxicity of different aggregate-prone proteins. *Hum. Mol. Genet. 15*, 433−442.
(31) Chai, Y., Koppenhafer, S. L., Bonini, N. M., and Paulson, H. L. (1999) Analysis of the role of heat shock protein (Hsp) molecular chaperones in polyglutamine disease. *J. Neurosci. 19*, 10338−10347.
(32) Lee, L. C., Chen, C. M., Chen, F. L., Lin, P. Y., Hsiao, Y. C., Wang, P. R., Su, M. T., Hsieh-Li, H. M., Hwang, J. C., Wu, C. H., Lee, G. C., Singh, S., Lin, Y., Hsieh, S. Y., Lee-Chen, G. J., and Lin, J. Y. (2009) Altered expression of HSPA5, HSPA8 and PARK7 in spinocerebellar ataxia type 17 identified by 2-dimensional fluorescence difference in gel electrophoresis. *Clin. Chim. Acta 400*, 56−62.
(33) Chen, C. M., Lee, L. C., Soong, B. W., Fung, H. C., Hsu, W. C., Lin, P. Y., Huang, H. J., Chen, F. L., Lin, C. Y., Lee-Chen, G. J., and Wu, Y. R. (2010) SCA17 repeat expansion: Mildly expanded CAG/CAA repeat alleles in neurological disorders and the functional implications. *Clin. Chim. Acta 411*, 375−380.
(34) Warrick, J. M., Chan, H. Y., Gray-Board, G. L., Chai, Y., Paulson, H. L., and Bonini, N. M. (1999) Suppression of polyglutamine-mediated neurodegeneration in *Drosophila* by the molecular chaperone HSP70. *Nat. Genet. 23*, 425−428.
(35) Cummings, C. J., Sun, Y., Opal, P., Antalffy, B., Mestril, R., Orr, H. T., Dillmann, W. H., and Zoghbi, H. Y. (2001) Over-expression of inducible HSP70 chaperone suppresses neuropathology and improves motor function in SCA1 mice. *Hum. Mol. Genet. 10*, 1511−1518.
(36) Skaggs, H. S., Xing, H., Wilkerson, D. C., Murphy, L. A., Hong, Y., Mayhew, C. N., and Sarge, K. D. (2007) HSF1-TPR interaction facilitates export of stress-induced HSP70 mRNA. *J. Biol. Chem. 282*, 33902−33907.
(37) Fujikake, N., Nagai, Y., Popiel, H. A., Okamoto, Y., Yamaguchi, M., and Toda, T. (2008) Heat shock transcription factor 1-activating compounds suppress polyglutamine-induced neurodegeneration through induction of multiple molecular chaperones. *J. Biol. Chem. 283*, 26188−26197.
(38) Tanida, I., Ueno, T., and Kominami, E. (2004) LC3 conjugation system in mammalian autophagy. *Int. J. Biochem. Cell Biol. 36*, 2503−2518.
(39) Jänen, S. B., Chaachouay, H., and Richter-Landsberg, C. (2010) Autophagy is activated by proteasomal inhibition and involved in aggresome clearance in cultured astrocytes. *Glia 58*, 1766−1774.
(40) Yang, F., Yang, Y. P., Mao, C. J., Liu, L., Zheng, H. F., Hu, L. F., and Liu, C. F. (2013) Crosstalk between the proteasome system and autophagy in the clearance of α-synuclein. *Acta Pharmacol. Sin. 34*, 674−680.
(41) Jimenez-Sanchez, M., Thomson, F., Zavodszky, E., and Rubinsztein, D. C. (2012) Autophagy and polyglutamine diseases. *Prog. Neurobiol. 97*, 67−82.
(42) Williams, A., Jahreiss, L., Sarkar, S., Saiki, S., Menzies, F. M., Ravikumar, B., and Rubinsztein, D. C. (2006) Aggregate-prone proteins are cleared from the cytosol by autophagy: therapeutic implications. *Curr. Top. Dev. Biol. 76*, 89−101.
(43) Menzies, F. M., Huebener, J., Renna, M., Bonin, M., Riess, O., and Rubinsztein, D. C. (2010) Autophagy induction reduces mutant ataxin-3 levels and toxicity in a mouse model of spinocerebellar ataxia type 3. *Brain 133*, 93−104.
(44) Kim, S. J., Kim, T. S., Hong, S., Rhim, H., Kim, I. Y., and Kang, S. (2003) Oxidative stimuli affect polyglutamine aggregation and cell death in human mutant ataxin-1-expressing cells. *Neurosci. Lett. 348*, 21−24.
(45) Kiffin, R., Christian, C., Knecht, E., and Cuervo, A. M. (2004) Activation of chaperone mediated autophagy during oxidative stress. *Mol. Biol. Cell 15*, 4829−4840.
(46) Bauer, P. O., Goswami, A., Wong, H. K., Okuno, M., Kurosawa, M., Yamada, M., Miyazaki, H., Matsumoto, G., Kino, Y., Nagai, Y., and Nukina, N. (2010) Harnessing chaperone-mediated autophagy for the selective degradation of mutant huntingtin protein. *Nat. Biotechnol. 28*, 256−263.
(47) Sidell, N. (1981) Retinoic acid-induced growth inhibition and morphologic differentiation of human neuroblastoma cells *in vitro*. *J. Natl. Cancer Inst. 68*, 589−596.
(48) Cheung, Y. T., Lau, W. K., Yu, M. S., Lai, C. S., Yeung, S. C., So, K. F., and Chang, R. C. (2009) Effects of all-*trans*-retinoic acid on

human SH-SY5Y neuroblastoma as *in vitro* model in neurotoxicity research. *Neurotoxicology 30*, 127−135.
(49) Chang, K. H., Chen, W. L., Wu, Y. R., Lin, T. H., Wu, Y. C., Chao, C. Y., Lin, J. Y., Lee, L. C., Chen, Y. C., Lee-Chen, G. J., and Chen, C. M. (2014) Aqueous extract of *Gardenia jasminoides* targeting oxidative stress to reduce polyQ aggregation in cell models of spinocerebellar ataxia 3. *Neuropharmacology 81*, 166−175.
(50) Humphrey, G. R., and Kuethe, J. T. (2006) Practical methodologies for the synthesis of indoles. *Chem. Rev. 106*, 2875−2911.
(51) Cacchi, S., and Fabrizi, G. (2011) Update 1 of: Synthesis and functionalization of indoles through palladium-catalyzed reactions. *Chem. Rev. 111*, PR215−PR283.
(52) Flis, S., and Splwinski, J. (2009) Inhibitory effects of 5-fluorouracil and oxaliplatin on human colorectal cancer cell survival are synergistically enhanced by sulindac sulfide. *Anticancer Res. 29*, 435−441.